Evolution of morphology, structure and emission in Si-rich HfO_2:Nd films with annealing times

A Rivero, T Torchynska, L Vega, J Casas, L Khomenkova, F Gourbilleau

Journal of Physics: Conference Series **1723** (2021) 012044 doi:10.1088/1742-6596/1723/1/012044

Evolution of Morphology, Structure and Emission in Si-rich HfO_2:Nd films with Annealing Times

A Rivero[1], T Torchynska[2], L Vega[3], J Casas[2], L Khomenkova[4] and F Gourbilleau[5]

[1]Instituto Politécnico Nacional, UPIITA, Av. IPN. México City, 07320, México
[2]Instituto Politécnico Nacional, ESFM, Av. IPN. México City, 07738, México
[3]Instituto Politécnico Nacional, ESIME, Av. IPN. Mexico City, 07738, Mexico
[4] V. Lashkaryov Institute of Semiconductor Physics at NASU, Kyiv, 03028, Ukraine
[5] CIMAP/ UMR CNRS/ CEA/ ENSICAEN/ UNICAEN, Caen Cedex 4, France

E-mail: leovegma@gmail.com

Abstract. The impact of the time at high temperature annealing on the morphology, crystal structure and emission in visible spectral range has been studied in Si rich HfO_2:Nd films produced by radio-frequency magnetron sputtering in pure argon plasma. The annealing was carried out at 900 °C for 1, 5, 10, 30 and 60 min in the nitrogen atmosphere. A set of experimental methods have been used, such as: scanning electron microscopy (SEM), energy dispersive X-ray spectroscopy (EDS), X-ray diffraction (XRD) and photoluminescence (PL). In the present work the joint analysis of PL and XRD results permits us to estimate the optimal time parameters of annealing at 900 °C the Si-HfO_2: Nd films for obtaining the bright emission via 4f electronic levels of the Nd ions embedded in the tetragonal HfO_2 phase mainly after long annealing (30- 60 min). The film oxidation for annealing times (60 min) stimulated some crystal phase transformation with the start of formation of the tetragonal SiO_2 phase, that is accompanied by the defect generation and decreasing the PL intensity. The discussion of PL and XRD results is presented in detail.

1. Introduction

The HfO_2 nanocrystal films are the interesting object for different applications, such as: the nuclear materials, high temperature o high pressure materials, as gate oxides or optical waveguide materials in electronics [1-2]. HfO_2 is characterized by the high melting temperature, extreme chemical inertness and the high cross section for the thermal neutron capture [1]. The early interest to hafnium dioxide was connected with improving the parameters of advanced complementary metal-oxide semiconductor (CMOS) integrated circuits by using this higher dielectric constants (k) material as gate oxides [2]. In addition, hafnium base gate oxide is interesting due to its high dielectric constant (≈25), large conduction band offset (1.5 eV) and compatibility with polysilicon technology [3]. Furthermore, the high refractive index (n=1.9-2.2) and high optical transparency in the UV-IR spectral ranges (band gap is nearly 5.8-6.0 eV) offer the optical applications for this oxide [4]. The low probability of phonon assisted non- radiative recombination makes the HfO_2 films attractive for doping by rare-earth elements.

[1] leovegma@gmail.com

A few groups reported on the light emission obtained from Eu^{3+}-doped HfO_2 nanotubes [5], Er^{3+}-doped sol-gel SiO_2- HfO_2 waveguides [6], as well as Nd^{3+}, Er^{3+} or Pr^{3+} doped HfO_2 thin films [7, 8]. The different host materials for Nd^{3+} ions were studied, such as the garnets [9], glasses [10], ceramics [11], II-VI compounds [12], Si-rich SiO_2 or Si_3N_4 [13].

In this work we present the results of the structural and spectroscopic study of the HfO_2-based thin films co-doped with Si and Nd and grown by radio frequency (RF) magnetron sputtering. The effect of annealing times at high temperature of 900 °C on the morphology, phase separation process and emission of such composite films has been studied, as a very informative way for monitoring the optical properties of HfO_2-based films.

2. Experimental details

The HfO_2 films were grown by RF magnetron sputtering on 2-inch, β-doped, (100) oriented Si wafers with a resistivity of about 15 Ω·cm. A pure HfO_2 target (99.9%) topped with the calibrated Si and Nd_2O_3 pellets was used. The Si and Nd_2O_3 pellets covered of 16 % of target surface each.

To produce the Si-HfO_2:Nd films, the deposition was performed in pure Ar plasma with argon flow f_{Ar}=3 sccm (so-called "standard" approach). The deposition time was 200 min allowed to grow the films with the thickness of 410 nm. The RF power density, substrate temperature, total plasma pressure and substrate-cathode distance were 0.74 W/cm^2, 400 °C, 0.03 mbar and 57 mm, respectively. After the film deposition, the substrate was divided onto a set of pieces (1×1 cm^2) to study the effect of annealing times. Annealing was performed in a conventional horizontal furnace at the temperatures T_A=900 °C for 1, 5, 10, 30 and 60 minutes in a continuous nitrogen flow (48 sccm).

To study the film surface morphology, as well as to get the information on their chemical composition, a scanning electronic microscope (SEM) Quanta 3D FEG-FEI with an additional detector Apollo X10 mark EDAX for the energy dispersive X-ray spectroscopy (EDS) was used.

X-ray diffraction (XRD) results were obtained using the equipment of Model X" PERT MRD with the Pixel detector, three axis goniometry and parallel collimator with the angular resolution of 0.0001 degree. X-ray beam was achieved from the Cu source ($K_{\alpha 1}$ line, λ=1.5406 Å). All experiments were carried out at the room temperature.

PL spectra were detected using a spectrometer SPEX 500 with a Hamamatsu photomultiplier. PL was excited by the 325 nm emission of a He–Cd laser (KIMMON Model: IK3102R-G) with an emission power 50 mW.

3. Experimental results and discussion

3.1. Chemical composition and surface morphology

The chemical composition of the films was analyzed by the EDS technique (shown in Table 1) and the representative spectra obtained for the films annealed at 1, 5, 10, 30 and 60 min are shown in Fig. 1a.

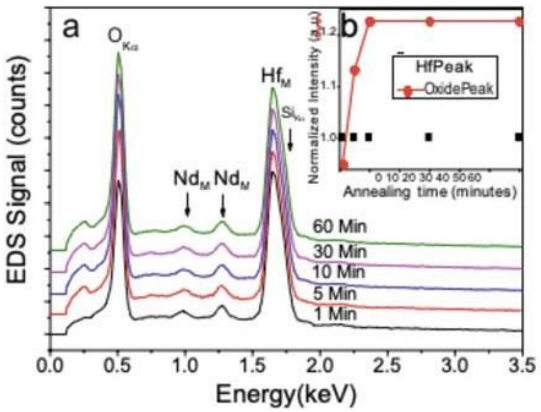

Figure 1. EDS spectra of annealed films

Table 1. Chemical composition of the films

Element	As deposit Atomic %	1 min Atomic %	10 min Atomic %	60 min Atomic %
NdM	1.1	1.07	1.05	1.03
HfM	29.05	28.81	27.15	27.32
SiKa	10.83	7.92	7.80	7.71
OKa	59.02	62.20	64.00	63.94

For all films, EDS spectra were found to be similar and included the peaks of Hf, Si, Nd and O elements. It is clear in figure 1b that the intensity of the peak Oka increased with increasing the annealed times. The growth of the peak Okα intensity in EDS spectra of annealed films can be caused by oxygen adsorption by the film surface at annealing treatment and oxygen diffusion inside film volume with the formation of Si-OX or Hf-O bonds. However, for $t \geq 10$ min, the oxygen out-diffusion can occur. This can result in the variation of the intensity of Oka signals that was observed for the films annealed at longer times.

The surface SEM images of the as-deposit and annealed films for: 1, 10 and 60 minutes, are presented in figure 2.

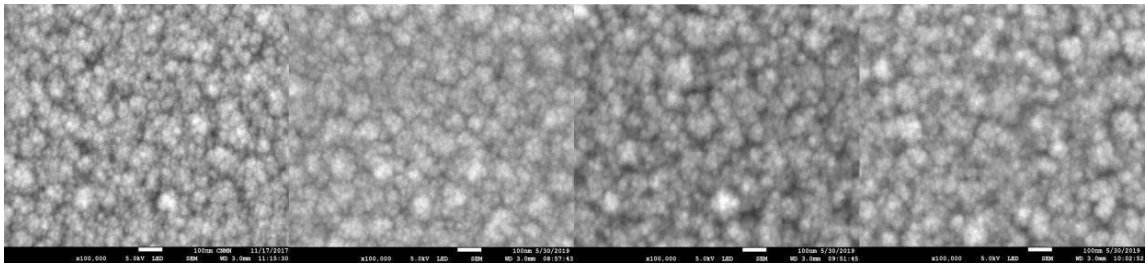

a. As deposit b. 1 minute c. 10 minutes d. 60 minutes

Figure 2. Surface SEM images of the films.

It is clear that the small nanocrystals (with the sizes below 20 nm) form large grains (about 40-60 nm) separated by the valleys. This morphology can be explained by the Structure Zone Model (SZM), It was shown early that for the most metals and dielectrics, the activation energies for the diffusion are connected with melting temperature of materials, T_M [14], and the effect of total plasma pressure on the film surface [15]. Thus, the process depends on T_S/T_M=0.1-0.3 (so-called after zone T in SZM model), the atom self-diffusion is appreciable and the formation of films with the dense array of grains separated by grain boundaries occurs owing sintering the grains [14].

In this research, substrate temperature was T_S=400 °C (673 K). As for melting point of Si-Nd_2O_3-HfO_2 composite target, one can consider that the main contribution will be given rather by HfO_2 target (T_M=2810- 2900 °C (3083-3173 K)) then Si pellets (T_M=1414 °C (1687 K)) and Nd_2O_3 ones (T_M=2233°C (2506 K)) due to its larger contribution in composite target. Thus, the ratio T_S/T_M ~0.21-0.22 is obtained that allows expecting the grain formation in the film annealed for 1min (Fig.1a). After film annealing for the 10 up to 60 min the sintering the grains occurs and their sizes increases up to 40-100 nm (Fig.1c, d).

3.2. XRD Study

XRD patterns recorded with the symmetric geometry for the films annealed at different times are shown in Fig. 3. The film annealed 1 min demonstrates a set of XRD peaks that can be attributed to the different phases (Fig.3, curve 1). The high intensity XRD peak at 2θ =69.173° (f) is identified as a XRD signal from the (400) planes in the cubic Si crystal structure (ICSD Ref. code 00-005-0490). This signal is related to the Si substrate. The XRD peak with the small intensity (Fig. 3, curves 1) detected at 2θ = 32.952° (a) was attributed to the diffraction from the (124) plane in the tetragonal Nd2Si2O7 phase (ICSD Ref code 01-089-5347). It is supposed that high enough substrate temperature (400 °C) can be favoured to the appearance of Nd2Si2O7 phases. Finally, the peak at 62.722° (8) is related to the diffraction on the (202) planes of a HfO2 phase.

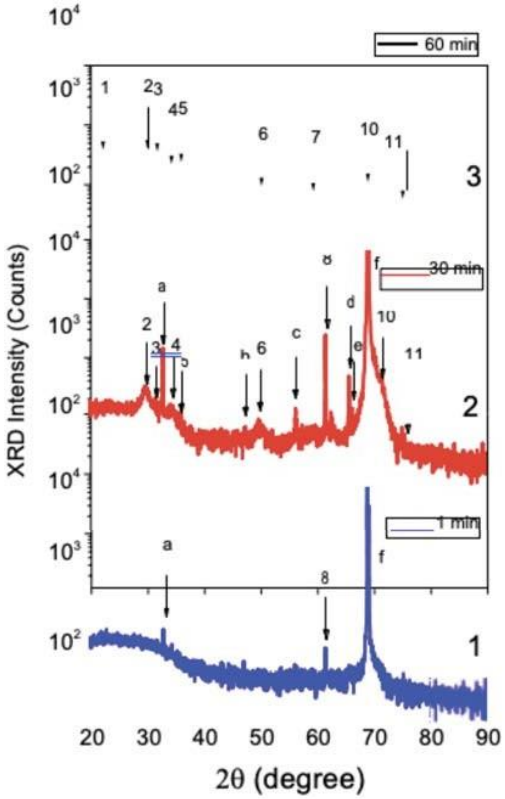

Figure 3. XRD spectra of Si-HfO2:Nd films: 1 minute (curve 1), 30 minutes (curve 2) and 60 minutes annealing time (curve 3).

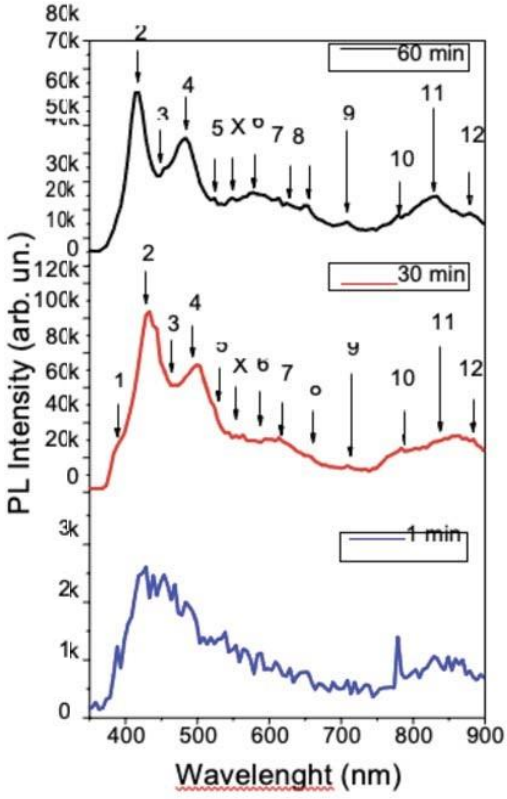

Figure 4. PL spectra of Si-HfO2:Nd films: 1 minute, 30 minutes and 60 minutes annealing time recorded in the visible spectral range.

Annealing the Si–HfO_2: Nd film for 30 min stimulates the structure variation (Fig. 3, curve 2). The new XRD signals at 2θ =32.952° (a) and 66.432° (e) have appeared. These peaks are related to the diffraction on the (124) and (133) planes in the tetragonal Nd_2Si2O7 phase (ICSD Ref. code 01-089-5347) Meanwhile, the XRD peaks at 2θ=47.532° (b), 56.412° (c), 65.892° (d), were attributed to the diffraction from the (103), (213) and (224) planes in the tetragonal HfSiO4 phase (ICSD Ref. code 01-077-1759, 00-008-0345 and 00-036-0088), respectively (Fig. 3, curve 2). At the same time, the XRD peaks connected with the tetragonal HfO2 phase were detected at 2θ = 34.132° (4), 49.352° (6), 62.722° (8) (Fig. 3, curve 2), related to the diffraction on (002), (202) and (113) planes in the tetragonal HfO_2 phase (ICSD Ref. code 00-008-0342, and 00-034-0104), respectively.

Annealing the Si–HfO_2:Nd film for 60 min stimulates the significant structure variation (Fig. 3, curve 3). The XRD signals from $Nd_2Si_2O_7$ and $HfSiO_4$ tetragonal phases disappeared (Fig. 3,

curve 3) that can be related to the decomposition of both these phases. At the same time, the XRD peaks connected with the tetragonal HfO_2 phase were detected at 2θ = 29.292° (2), 34.132° (4), 49.352° (6) and 59.632° (7) (Fig. 3, curve 3). These peaks are related to the (101), (002), (202) and (311) planes in the tetragonal HfO_2 phase (ICSD Ref. code 00-008-0342), respectively. Additionally, the peak 9 shifts towards 2θ = 69.272° (9) due to its overlapping with the XRD peak at 2θ = 70.603° (peak 9) (Fig. 3, curve 3). The last one can be assigned to the X-ray diffraction from a (002) plane in the tetragonal SiO_2 phase (ICSD Ref. code 00-045-1374). Finally, there is a peak at 2θ = 22.352° related to the diffraction on the Si (400) planes (ICSD Ref. code 00-005-0490).

Annealing at higher annealing time (60 min) stimulates the silicon oxide crystallization in the studied films that is accompanied by appearing the other set of XRD peaks at 2θ = 30.192° (3) and 36.132° (5) that correspond to the diffraction on the (110) and (411) planes in the tetragonal SiO_2 phase (ICSD Ref. code 00-045-1374).

3.3. PL Study

PL spectra of the Si–HfO_2: Nd films annealed for 1, 30 and 60 min are shown in Fig. 4. The total PL intensity increases significantly after 30 min annealing, but it decreases slightly after 60 min annealing in comparison with 30 min annealing (Fig. 4). PL spectra consist of the several PL bands related to the optical transition in the 4f inner electronic shell of Nd^{3+} ions with the peaks (1–13) in the spectral range of 350–900 nm (Fig. 4, Table 2). Additionally, the PL peak X has been detected and assigned to emission via native host defects (Fig. 5, Table 2). It is clear that the contribution of Nd^{3+} ions and host defects in film emission depends on annealing time and on the crystal phase of host matrix (Table 2, Fig. 4, Fig. 5).

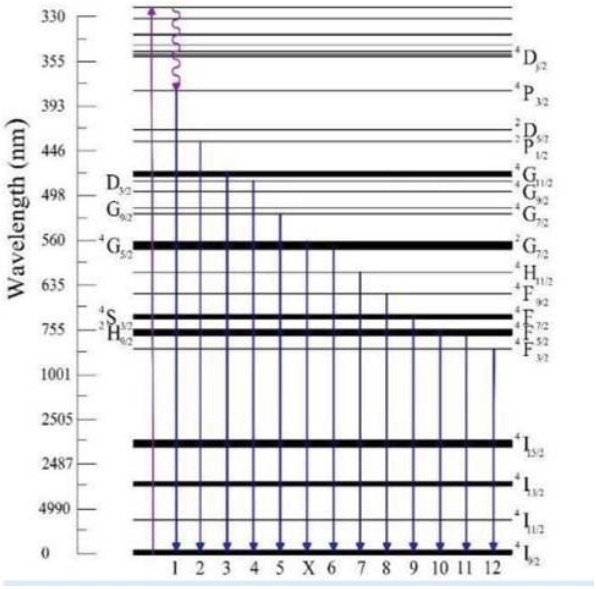

Figure 5. Excitation and recombination optical transitions via the 4f inner electronic levels detected for the Nd^{+3} ions embedded in Si- HfO_2:Nd films.

Table 2. Optical transitions detected in the films (Figure 4).

Number	Wavelength	Optical transition	Ref.
1	390	$^4P_{3/2} \rightarrow {}^4I_{9/2}$	[18]
2	420	$^2P_{1/2} \rightarrow {}^4I_{9/2}$	[18]
3	455	$^4G_{11/2} \rightarrow {}^4I_{9/2}$, $^4G_{9/2} \rightarrow {}^4I_{9/2}$	[19]
4	480	$^4G_{9/2} \rightarrow {}^4I_{9/2}$	[15]
5	525	$^4G_{7/2} \rightarrow {}^4I_{9/2}$	[19]
X	555	Vo	[16, 17]
6	590	$^2G_{7/2}$ C $^4I_{9/2}$	[17]
7	625	$^4H_{11/2}$ C $^4I_{9/2}$	[19]
8	655	$^4F_{9/2}$ C $^4I_{9/2}$	[18]
9	710	$^4F_{7/2}$ C $^4I_{9/2}$	[18]
10	760	$^4H_{9/2}$ C $^4I_{9/2}$	[18]
11	800	$^4H_{7/2}$ C $^4I_{9/2}$	[18]
12	885	$^4F_{3/2}$ C $^4I_{9/2}$	[15, 20]

It was shown early that the emission of pure HfO_2 is characterized by the PL bands in the ultraviolet (4.0–4.2 eV) and visible (2.2–3.5 eV) spectral ranges [16, 17]. The UV emission was attributed either to the emission of the self-trapped exciton or to oxygen vacancies. Since the exciton emission is usually quenched to 300 K, the most probable center for UV emission are oxygen vacancies. Along with this, visible emission at 300 K was attributed to the carrier recombination via oxygen vacancies with trapped electrons [16, 17]. In present study, the band X in the range 400-555 nm (≈2.2-3.1 eV), which appeared after 1min annealing (Fig. 4), can be attributed to the optical transitions via different types of oxygen vacancies. The highest PL intensity is detected in the PL spectrum of the film annealed for 30 min. In the latter case the film crystal structure is characterized by the tetragonal HfO_2 phase mainly (Fig.3). The nature of optical transitions related to the electronic shell of the Nd ions is summarized in Table 1. The film oxidation while annealing for 60 min is accompanied by some crystal phase transformation with appearing the tetragonal SiO_2 phase (Fig. 3). The last process stimulates, apparently, the generation of nonradiative defects that decreases the PL intensity of the films (Fig.4).

4. Conclusions

The effects of annealing time at T=900 °C on light emission, chemical composition and structural properties of the Si rich HfO_2:Nd films have been investigated. It is shown that annealing at T=900 °C for 30-60 min stimulates the formation of the nanocrystal tetragonal HfO_2 phase mainly and appearance of the bright emission related to the optical transitions in the 4f inner electronic shell of Nd^{3+} ions. In addition, we revealed the optimal parameters (temperature and time) of the annealing Si-HfO_2:Nd films for obtaining the bright emission via 4f electronic levels in the Nd ions embedded in the tetragonal HfO_2 phase mainly after long time annealing. The optimal parameters are: 900 °C and 30 min.

Acknowledgments

This work was partly supported by National Academy of Sciences of Ukraine (project III-4-16), Ministry of Education and Science (project ID: 89452), the French National Agency of Research

(ANR), as well as by the CONACYT Mexico (project 258224) and SIP, IPN Mexico (project 20201337, 20201886, 20200446).

References

[1] K Komarek, P Spencer and International Atomic Energy Agency 1981 Atomic Energy Review *Special International Atomic Energy Agency* **8** 245
[2] S Ramanathan, P McIntyre, J Luning, P Lysaght, Y Yang, Z Chen, and S Stemmer 2003 Electrochem. *Soc.* **150(10)** F173– F177
[3] J Robertson 2006 *Reports on Progress in Physics* **69** 327-396
[4] L Khomenkova, X Portier, J Cardin and F Gourbilleau 2010 *Nanotechnology* **21** 1231-1235
[5] X Liu, Z Ma, Y Xie, Y Su, H Zhao, M Zhou, J. Zhou and E. Xie 2010 *Appl Phys* **1071** 5
[6] N Afify, G Dalba, F Rocca 2009, *J. Phys. D: Appl. Phys.* **42** 115416 1-11
[7] L Khomenkova, Y An, D Khomenkov, X Portier, C Labbé and F Gourbilleau 2014 *Physica B: Condensed Matter* **453** 100-106
[8] L Vega, T Torchynska, L Khomenkova and F Gourbilleau 2019 *Mater. Chem. and Physics.* **229** 263-268
[9] V Monteseguro, M Rathaiah, K Linganna, A Lozano-Gorrín, MHernández-Rodríguez, Martín and P Babu 2015 *Optical Materials Express* **5** 1661-1673
[10] E Serqueira, N Dantas 2014 *Optics Letters* **39** 131-134
[11] G Yi, W Li, J Song, B Mei, Z Zhou, L Su 2018 *J. European Ceramic Society* **38** 3240-3245
[12] M Balestrieri, S Colis, M Gallart, G Ferblantier, D Muller, P Gilliot, P Bazylewski, G Chang, A Slaouib, A Dinia 2014 *J. Mater. Chem.* **C2** 9182-9188
[13] P Pirasteh, J Charrier, Y Dumeige, J Doualan, P Camy, O Debieu, H Liang, L. Khomenkova, J Lemaitre, F Gourbilleau 2013 *J. Appl. Phys.* **114 014906** 1- 6
[14] B Movchan, A Demchishin 1969 *Fiz. Metal. Metalloved* **28** 653-660
[15] Thornton 1974 *J. Vac. Sci. Technol.* **11** 666-670
[16] J Khomenkova, Y An, D Khomenkov, X Portier, C Labbé, F Gourbilleau 2014 *Phys B* **453** 100-106.
[17] R Demoulin, G Beainy, C Castro, P Pareige, L Khomenkova, C Labbé, F Gourbilleau, E Talbot 2018 *Nano Futures* **2 035005** 1-12
[18] C Liang, O Debieu, Y An, L Khomenkova, J Cardin, F Gourbilleau 2012 *J. Lumin.* **132** 3118-3121
[19] G Yi, W Li, J Song, B Mei, Z Zhou, L Su 2018 *J. Eur. Ceram. Soc.* **38** 3240-3245
[20] M Balestrieri, S Colis, M Gallart, G Ferblantier, D Muller, P Gilliot, P Bazylewski, G Chang 2014 *J. Mater. Chem.* **C2** 9182-9188